

Activation of the c-Met Receptor Complex in Fibroblasts Drives Invasive Cell Behavior by Signaling Through Transcription Factor STAT3

Alexander Cramer,¹ Sandra Kleiner,¹ Martin Westermann,² Anja Meissner,¹ Anika Lange,¹ and Karlheinz Friedrich^{1*}

¹Institute of Biochemistry I, Friedrich Schiller University Jena, Nonnenplan 2, 07743 Jena, Germany

²Centre of Electron Microscopy, Friedrich Schiller University Jena, Ziegelmühlenweg 1, 07743 Jena, Germany

Abstract c-Met is the receptor for hepatocyte growth factor/scatter factor (HGF/SF). It mediates multiple cellular responses in development and adult life, and c-Met hyperactivity is associated with malignant transformation of cells and the acquisition of metastatic properties. Signal transducer and activator of transcription 3 (STAT3) has been shown to contribute to c-Met-mediated cell motility and is, thus, potentially involved in the control of invasive cell behavior. We have functionally reconstituted c-Met-dependent signal transduction in fibroblasts with the aim of studying Met-driven cell invasiveness and the role of STAT3 in this phenomenon. Activation of the system was achieved by means of a hybrid receptor comprising the extracellular domain of the nerve growth factor (NGF) receptor TrkA, the cytoplasmic part of c-Met and a C-terminally fused blue fluorescent protein (BFP). In addition, a GFP-tagged derivative of adaptor protein Gab1 was expressed. NGF-stimulation of mouse fibroblasts expressing tagged versions of both Trk-Met and Gab1 with NGF resulted in anchorage-independent growth and enhanced invasiveness. By freeze-fracture cytochemistry and electron microscopy, we were able to visualize the ligand-induced formation of multivalent receptor complex assemblies within the cell membrane. NGF-stimulation of the heterologous receptor system evoked activation of STAT3 as evidenced by tyrosine phosphorylation and the formation of STAT3 clusters at the cell membrane. siRNA-mediated ablation of STAT3 expression resulted in a drastic reduction of c-Met-driven invasiveness, indicating an important role of STAT3 in the control of this particularly relevant property of transformed cells. *J. Cell. Biochem.* 95: 805–816, 2005. © 2005 Wiley-Liss, Inc.

Key words: c-Met; STAT3; invasiveness; receptor activation

The malignancy of tumor cells is associated with their ability to invade into surrounding tissues and through tissue boundaries and to ultimately give rise to metastases. The complex molecular mechanisms involved in the acquisi-

tion of invasiveness are only partly understood, but encompass in their early stages the activity of growth factor receptors and cytoplasmic signal mediators [Wells et al., 2002].

Transmembrane tyrosine kinase c-Met, the receptor for hepatocyte growth factor/scatter factor has, apart from multiple physiological functions [Rubin et al., 1993], oncogenic properties including the stimulation of cell dissociation, migration, motility, and invasion of extracellular matrix [e.g., Rong et al., 1994; Jeffers et al., 1996; Sachs et al., 1996; Otsuka et al., 1998]. Various intracellular substrates of c-Met and their respective downstream pathways have been implicated in the signaling processes towards invasive cell behavior, i.e., adapter proteins Gab1 [Maroun et al., 1999] and Grb2 [Atabey et al., 2001], Src-kinase [Rahimi et al., 1998], and phosphoinositol-3 kinase [Kotelevets et al., 1998]. However, attempts to correlate specific oncogenic effects with the

Grant sponsor: Deutsche Forschungsgemeinschaft (to KF); Grant number: FR 854/4-1; Grant sponsor: Interdisziplinäres Zentrum für Klinische Forschung (IZKF) at the University of Jena.

Sandra Kleiner's present address is Friedrich Miescher Institute for Biomedical Research, Maulbeerstrasse 66, 4058 Basel, Switzerland.

*Correspondence to: Dr. Karlheinz Friedrich, Institute of Biochemistry, Friedrich-Schiller-University Jena, Nonnenplan 2, 07743 Jena, Germany. E-mail: khf@mti.uni-jena.de

Received 25 August 2004; Accepted 24 January 2005

DOI 10.1002/jcb.20459

© 2005 Wiley-Liss, Inc.

individual activities of these signaling mediators have not yet yielded a clear picture. These difficulties are in part due to the facts that various signaling pathways emanate from a common "bidentate" phosphorylated docking site within the cytoplasmic domain of activated c-Met [Ponzetto et al., 1994] and that c-Met effectors probably compete for this multisubstrate binding site and can become activated both by direct and indirect interactions within the receptor complex [e.g., Lock et al., 2000; Schaefer et al., 2002].

Signal transducer and activator of transcription STAT3 is one of the c-Met substrates that become phosphorylated upon receptor activation and has received much attention in the last years as an emerging player in various aspects of oncogenesis and as a potential target for anti-tumor drugs. Importantly, STAT3 was shown to be essential for HGF-induced morphogenesis. This process involves an increase of directed motility and is, thus, related to c-Met-driven invasive cell behavior [Boccaccio et al., 1998]. STAT3 has multiple functions in development and throughout the adult organism [reviewed by Levy and Lee, 2002] and is crucial for various processes that include cell migration, e.g., in the course of germ cell invasion [Li et al., 2003], gastrulation [Yamashita et al., 2002], or keratinocyte movement during wound healing [Sano et al., 1999]. We have recently observed that STAT3 activation in trophoblast cells ceases during the course of pregnancy in temporal correlation with their loss of invasive properties [Corvinus et al., 2003].

Dysregulated STAT3 activation was found in various cancers [e.g., Garcia et al., 2001; Dhir et al., 2002; Schaefer et al., 2002] and it has also been associated with tumor metastasis [Horiguchi et al., 2002]. While the molecular mechanisms connecting aberrant STAT3 activity and malignant cell properties are as yet poorly defined, STAT3 was proven to be capable of directly causing malignant cell transformation, i.e., to act as a bona fide oncoprotein [Bromberg et al., 1999].

Inhibition of STAT3 signaling appears to have attractive perspectives for the therapeutic interference with malignant properties of tumor cells. Suppression of STAT3 activity, for instance, can block c-Met-mediated tumorigenic growth of leiomyosarcoma cells *in vitro* as well as in athymic mice [Zhang et al., 2002]. Interestingly, blockade of STAT3 reduced the

motility of ovarian cancer cells whose aggressive clinical behavior showed a correlation with constitutively active STAT3 levels [Silver et al., 2004].

Employing a reconstituted c-Met receptor complex in murine fibroblasts, we have addressed the contribution of STAT3 signaling for c-Met-induced invasiveness. We show that siRNA-mediated knockdown of STAT3 profoundly reduces c-Met-driven invasive cell behavior. Signal transduction via STAT3 is, thus, an important component of the pathway(s) leading from c-Met activation to the acquisition of invasive cell properties.

MATERIALS AND METHODS

DNA Constructs

The Trk-Met-BFP construct was generated as follows: from a cDNA encoding the Trk-Met hybrid (a gift from Dr. M. Sachs, consisting of the extracellular domain of human TrkA and the transmembrane and cytoplasmic domain of murine c-Met [Sachs et al., 1996], a 3.0 kb Hind III/Xho I fragment comprising the entire reading frame was excised and cloned into the respective sites of pcDNA3.0 (Invitrogen, Carlsbad, CA) to yield pcDNA-TM. Subsequently, a 0.7 kb Bst XI/Xba I fragment representing the 3'-end of the cDNA was replaced with a Bst XI/Xba I PCR fragment encoding the carboxy-terminal part of murine c-Met fused to the linker GSIPA and the blue fluorescent protein (BFP). The latter fragment was obtained by recombinant PCR from two overlapping fragments derived from c-Met and BFP. The c-Met-derived fragment was produced employing the primers met-5'/BstX2 (5'-GGTTGCTGATTTC-GGTCTTGC-3') and linker-3'/met (5'-GGCTG-GAATCGATCCTGTGTTCCCTCGCCATC-3'). The BFP-fragment was generated from plasmid pQBI50 (Clontech, Palo Alto, CA) as template using the primers 3'/BFP-Xba (5'-GATGTCTA-GATTATTTGTATAGTTCATCC-3') and linker-5'/BFP (5'-GGATCGATTCCAGCCATGGCTAG-CAAAGGAGAAG-3'). Combination of the two primary fragments in a PCR with the primer pair 5'/BstX2/3'/BFP-Xba resulted in the final product which was cleaved with Bst XI and Xba I and ligated into the respective sites of pcDNA-TM to yield pcDNA-TM-BFP. The Gab1 fusion with destabilized enhanced GFP (d2EGFP) was generated as follows: from a cDNA encoding human Gab1 [Weidner et al., 1996, a gift from

Dr. M. Sachs] as template, a PCR fragment with terminal Nhe I and Bam HI sites was synthesized using primers SK1 (5'-ACTAGCTAGCACGCGTGCCGCGCATGAGCGGTGGTGAAGTGTCTGC-3') and SK2 (5'-AGATGGATCCGCTTTCACATTCTTTGTGGGTGTCTCGGACTCTGTGGA-3') and ligated in between the Nhe I and Bam HI site of pd2EGFP-N1 (Clontech). From the resulting plasmid pd2EGFP-Gab1, an Mlu I/Xba I fragment encoding a fusion of Gab1 and eGFP with the intervening linker sequence ADPPVAT was excised and used to replace the GFP insert of pBI-4-GFP- Δ Xba in between the respective sites. The resulting expression construct was named pBI-Gab1-EGFP. pBI-4-GFP- Δ Xba is a derivative of pBI-4-GFP [Friedrich and Wietek, 2001], in which the Xba I site immediately downstream of the SV 40 promoter had been removed by partial Xba I digestion, a fill-in reaction and relegation to obtain a vector with a unique Xba I site.

Cell Line, Cell Culture, and Transfection

The murine fibroblast cell line NIH 5.15 is a tetracycline-regulatable "tet-off" derivative of NIH 3T3 [Kerckhoff et al., 1998] and was obtained from Dr. J. Troppmair. Cells were cultured in Dulbecco's modified Eagle's medium supplemented with 10% fetal calf serum (heat inactivated at 56°C for 45 min), 2 mM L-glutamine, and 0.1 mg/ml gentamycin at 37°C in humidified air with 5% CO₂.

For transfection, cells were grown to 80% confluence in 6 cm² dishes. Cells were overlaid for 5 h with 1 ml serum-free DMEM containing 2.5 μ g of expression construct pcDNA-TM-BFP and/or pBI-Gab1-EGFP plus (in case of stable transfections) ptgCMV/HyTK [Lischke et al., 1995] and 10 μ l LipofectAMINE (Gibco, Carlsbad, CA) followed by transfer to fresh medium. For the generation of stable clones, 3 days after transfection cells were diluted into medium supplemented with 150 μ g/ml Hygromycin B (Serva, Heidelberg, Germany) and the cell suspension was aliquoted to 12-well plates. Hygromycin-resistant clones were expanded and analyzed for expression by Western blot.

Cell Lysis, Immunoprecipitation, SDS-PAGE, and Western Blotting

Cells were suspended in 100 μ l lysis buffer (20 mM HEPES pH 7.5, 2 mM EGTA, 0.2 mM EDTA, 0.12M NaCl, 1% Triton) supplemented with protease inhibitors (20 μ g/ml aprotinin

(trasyolol), 20 μ g/ml leupeptine, 5 μ g/ml pepstatin A, 647 ng/ml antipain, 10 μ g/ml bestatine, 0.1 mM PMSF, 1 mM sodium orthovanadate) at a density of 2×10^7 cells/ml. Protein concentrations of cell lysates were determined using a kit based on the Bradford method (Sigma, Taufkirchen, Germany).

Extracts were either employed directly for electrophoretic separation (see below) or subjected to immunoprecipitation (Ip). For Ip, 400 μ g of cell lysate was incubated with 4 μ g of anti-human Gab1 (sc-6292, Santa Cruz) or anti-mouse-Met SP260 (sc-162, Santa Cruz), respectively along with 50 μ l of affinity matrix solution (anti-goat-IgG-Agarose or Protein A-Agarose, both from Sigma) in a total volume of 1 ml lysis buffer. Antigen absorption, washing and collection of affinity beads was carried out as described [Kammer et al., 1996].

Gel electrophoresis and Western blotting was performed as published previously [Kammer et al., 1996]. Briefly, 20 μ g of whole cell extract or the collected affinity matrix after immunoprecipitation (see above) were solubilized in gel loading buffer (62.5 mM Tris/HCl pH 6.8; 2% SDS; 25% glycerol; 1% phenol blue; 5% β -mercaptoethanol), boiled for 10 min and separated on 6% acrylamide SDS gels. After protein transfer, nitrocellulose membranes were blocked in NET-G buffer (150 mM NaCl, 5 mM EDTA, 50 mM Tris/HCl pH 7.5, 0.05% Triton X-100, 0.2% Gelatine) for 1 h. Antibodies were applied for 36 h at the following dilutions: anti-GFP(FL) (sc-8334, Santa Cruz): 1:1,000, anti-phosphotyrosine (PY-99, sc-7020, Santa Cruz): 1:4,000, anti-human Gab1 (sc-6292, Santa Cruz): 1:100, anti-STAT3 p-Tyr705 (Cell Signaling Technology): 1:1,000, anti-STAT3 (c-20, Santa Cruz): 1:1,000, anti-mouse-Met SP260 (sc-162, Santa Cruz, Santa Cruz, CA): 1:1,000. For detection, peroxidase-conjugated anti rabbit IgG (Roth) was employed at a dilution of 1:10,000 for 1 h. Visualization was performed using an enhanced chemiluminescence (ECL) detection kit (Amersham). Removal of bound antibody for re-detection with an additional antibody was carried out by treating membranes twice for 20 min with 62.5 mM Tris/HCl pH 6.7, 2% SDS, 10 mM β -mercaptoethanol at 68°C and intermittent and final washing in $10 \times$ PBS at ambient temperature.

Densitometric quantification of band intensities was performed using Scion Image[®] software (Scion Corporation, Frederick, MD).

Soft Agar Colony Formation Assay

The soft agar assay measuring anchorage-independent growth has been reported elsewhere [Li et al., 1996]. Briefly, 10^5 NIH 5.15-derived cells were suspended in 4 ml of DMEM supplemented with 10% calf serum and 0.4% Seaplaque agarose in 6 cm² tissue culture plates containing 4 ml of a DMEM underlay with 0.8% agarose. Cultures were fed with 0.2 ml of DMEM containing 10% of fetal calf serum twice a week for 2 weeks. The colonies were stained with *p*-iodonitrotetrazolium violet (Sigma) after 2 weeks and photographed.

In Vitro Cell Invasion Assay

Cell invasiveness was quantified by a modified Boyden chamber method using polycarbonate transwells (Corning Costar Corp., Cambridge, MA) consisting of a separate top well, a filter (pore size 8 μ m, diameter 24 mm) and a corresponding lower well. Membrane filters were coated with 200 μ l of a 1:50 Matrigel (Becton Dickinson, Bedford, MA) dilution in ice-cold serum-free DMEM medium (40 μ g/filter) and dried overnight at 37°C. 2×10^5 exponentially growing cells (if transiently transfected after a recovery period of 48 h) in a volume of 1 ml serum-free medium (optionally containing 50 ng/ml NGF and/or 1 μ g/ml doxycycline) were seeded on top of a transwell. The lower compartment of each transwell unit contained 2.5 ml medium supplemented with 20% fetal calf serum. After incubation for 24 h at 37°C, medium with remaining cells and the matrigel layer were removed from the upper compartment of the transwells. Cells attached to the membranes were washed off by rinsing membranes twice with a total of 1 ml PBS containing 0.02% EDTA and 0.05% (w/v) trypsin. Washing solution was combined with the medium in the lower transwell compartment (containing cells that had already passed the membrane), and cells were collected by 10 min centrifugation at 1,000*g*. Cell pellets were resuspended in 1 ml of medium and stained with trypan blue. Migrated cells were quantified by counting of five random microscopic fields using a light microscope and a Neubauer chamber and extrapolation of the mean to the original volume of cell suspension. The percentage of invasive cells was expressed by relating the total number of migrated cells to the number of cells originally applied to the top of the transwell, which was set 100%.

Introduction of siRNA Into Fibroblasts

Purified RNA oligos were purchased from Ambion, Austin, TX. The oligonucleotide sequences of the STAT3 siRNA were: STAT3sense: 5'-UGUUCUCUAUCAGCACAAUTT-3', STAT3antisense: 5'-AUUGUGCUGAUAGAGAAC-ATT-3'. "Scrambled" control sequences were: SCRsense: 5'-GCCACUUAUAAUUCGUUCTT-3', SCRantisense: 5'-GAACGAAUUUAUAAAG-UGGCTT-3'.

siRNAs and controls were transfected into NIH-TM-BFP/Gab1-EGFP cells by "nucleofection" [Gresch et al., 2004]. Cells were plated and grown to confluence. They were harvested with 0.5% trypsin/0.02% EDTA in PBS and 1.5×10^6 cells were resuspended in 100 μ l of Nucleofector Solution R (Amaxa, Bergisch-Gladbach, Germany) containing 50 nM of siRNA oligonucleotides and 2.5 μ g GFP tracer plasmid (Amaxa) to monitor transfection efficiency. Cell suspensions were subjected to "nucleofection" in a Nucleofector apparatus (Amaxa), employing program A-24. Cells were then transferred to 6-well tissue culture plates, supplied with 2.5 ml of fresh prewarmed medium supplemented with 20% FCS and further grown for up to 8 days. At days 3 and 8, aliquots of transfectants were harvested and subjected to Western blot and invasiveness assays. Experiments were continued only if apparent transfection efficiency was above 50% as fluorescence microscopically determined by GFP expression 48 h post transfection.

Freeze-Fracture Preparation

Confluently grown NIH 5.15 cells transiently transfected with both pcDNA-TM-BFP and pBI-Gab1-EGFP were washed twice with PBS at growth temperature and carefully abraded from the culture dishes. Aliquots of the chemically unfixed cell suspension were enclosed between two 0.1 mm thick copper profiles as used for the sandwich double-replica technique. The sandwiches were physically fixed by rapid plunge freezing in liquid ethane/propane mixture, cooled by liquid nitrogen. Freeze-fracturing was performed in a BAF400T freeze-fracture unit (BAL-TEC, Liechtenstein) at -150°C using a double-replica stage. The fractured samples were shadowed without etching with 2–2.5 nm Pt/C (platinum/carbon) at an angle of 35°. The evaporation of Pt/C with electron guns was controlled by a thin-layer quartz crystal monitor.

Freeze-Fracture Immunogold-Labeling

For freeze-fracture immunogold-labeling and subsequent electron microscopy the freeze-fracture replica were transferred to a "digesting" solution (2.5% SDS in 10 mM Tris buffer pH 8.3 and 30 mM sucrose) and incubated over night according to Fujimoto [1997].

The replica were washed four times in PBS to remove SDS and treated for 30 min with PBS + 1% bovine serum albumin (BSA) and then placed onto a drop of an 1:50 diluted solution of antibody to human Gab1 or STAT3 (sc-6292 or sc-7179, polyclonal goat IgG, Santa Cruz Biotechnologies, Santa Cruz) in PBS with 0.5% BSA for 1 h. The replica were washed subsequently four times with PBS and placed on an 1:50 diluted solution of the second gold-conjugated antibody (goat anti goat IgG with 10 nm gold, British Biocell International, Cardiff, UK) in PBS with 0.5% BSA for 1 h. After immunogold-labeling, the replica were immediately rinsed several times in PBS, fixed with 0.5% glutaraldehyde in PBS for 10 min at room temperature, washed four times in distilled water and finally picked onto Formvar-coated grids for viewing in an EM 902A electron microscope (Zeiss, Oberkochen, Germany). Freeze-fracture micrographs were preferentially mounted with direction of platinum shadowing from bottom-up.

RESULTS

Functional Reconstitution of a Doubly Tagged c-Met Receptor Complex

We aimed at studying the activation process and oncogenic signal transduction of the c-Met receptor complex in a background-free fashion. Moreover, we were interested in following the formation of a signaling-competent assembly in dependence of ligand stimulation. For this purpose, we generated expression constructs encoding derivatives of both a c-Met/NGF receptor hybrid (Trk/Met) and the intracellular Met-effector Gab1 with carboxyterminally fused fluorescent proteins (Fig. 1A). Trk/Met is able of transmitting a c-Met-specific signal into cells upon activation with NGF [Sachs et al., 1996]. The Gab1-derived construct was placed under the control of a tetracycline-regulatable promoter, since we intended to alter experimentally the interaction equilibrium of c-Met effectors competing for the multisubstrate docking site

within the intracellular domain of activated c-Met. To favor independent folding and to minimize potential structural interference between the fusion partners, flexible linkers of five or seven amino acid residues, respectively, were inserted carboxy-terminally of the fluorescent protein moieties. Transient transfection of the two constructs into NIH 5.15 fibroblasts (expressing the Tet repressor, thus perspective-ly allowing for the experimental repression of Gab1-EGFP expression, see above) resulted in appearance of blue or/and green fluorescence as monitored by flow cytometry and fluorescence microscopy (data not shown). Expression and activity was studied biochemically by Western blot analysis of lysates from transfected cells that were either left unstimulated or treated with NGF (Fig. 1B). Since both c-Met and Gab1 are considered activators of invasive cell behavior, we studied the effects of transient expression of c-Met and Gab1 fusion constructs on invasiveness in vitro (Fig. 1C).

Antibodies to GFP (recognizing both BFP and EGFP) and human Gab1 confirmed expression and integrity of both fusion proteins. Trk-Met-BFP appeared in two forms of 190 and 160 kDa in size which represent the precursor and the mature receptor derivative. Probing blots with anti-phosphotyrosine showed that overexpression alone did already evoke a substantial grade of tyrosine phosphorylation of Trk-Met-BFP, probably due to some degree of spontaneous dimerization as a consequence of overexpression. Phosphorylation, however, was still enhanced by NGF stimulation, as evidenced by densitometric quantification of the relevant bands in Figure 1B. Phosphorylation of Gab1-EGFP was dependent on the simultaneous expression of the c-Met kinase as a constituent of Trk-Met-BFP and followed its activity pattern. Basal cell invasiveness of NIH 5.15 fibroblasts was clearly influenced by transient expression and activation of the heterologous Trk-Met-BFP/Gab1-EGFP system (Fig. 1C). Whereas expression of Trk-Met-BFP had no effect on the invasiveness of NIH 5.15 cells, activation of the receptor by NGF almost doubled the fraction of transmigrated cells in comparison to the parental cell line. Interestingly, additional expression of Gab1-EGFP further enhanced invasiveness. The effect was already evident in the absence of NGF stimulation and very profound upon stimulation of the c-Met receptor.

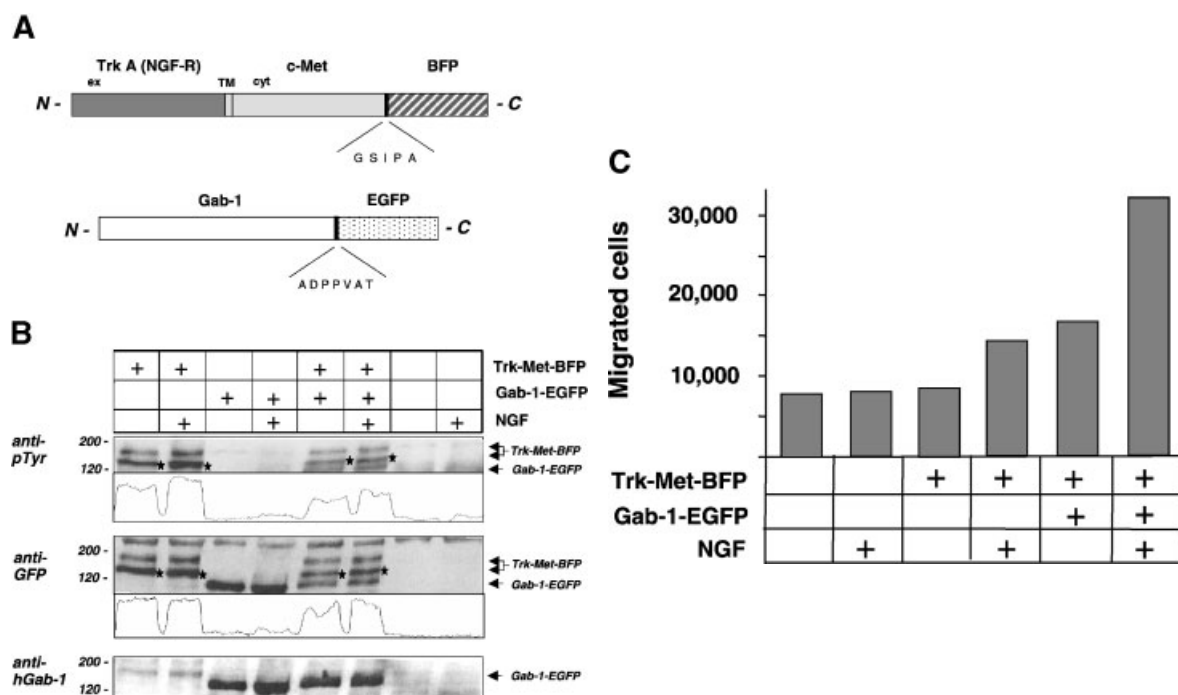


Fig. 1. Structure and functional expression of the fluorescence-tagged c-Met-derived receptor complex. **A:** Schematic depiction of the fusion proteins employed in this study. The BFP-tagged Trk-Met receptor hybrid (**top**) consists of the extracellular domain ("ex") of the human NGF receptor Trk A (dark gray), the transmembrane ("TM") and cytoplasmic domain ("cyt") of murine c-Met (light gray), a peptide linker (black) and blue fluorescent protein (BFP, striped). EGFP-tagged Gab1 (**bottom**) consists of the human Gab1 polypeptide (white) fused via a peptide linker (black) to destabilized enhanced GFP (d2EGFP, dotted). **B:** Examination of lysates from transfected and non-transfected NIH 5.15 cells for expression and phosphorylation of Trk-Met-BFP and Gab1-EGFP by Western blotting. Cells were transfected as indicated with expression constructs for the two tagged proteins and either left untreated or stimulated with NGF for 24 h. Samples were separated by PAGE, transferred to nitrocellulose and consecutively probed with an antibodies to phosphotyrosine (pTyr), GFP (recognizing both BFP and EGFP), and human Gab1.

These results indicate that the doubly tagged receptor system is functional in NIH 5.15 cells and drives cell invasiveness, in important parameter of cellular malignancy. They are also consistent with the view that both the activated c-Met receptor and its substrate Gab1 are involved in the mediation of invasive cell behavior.

Activation of c-Met Leads to the Formation of Multimeric Clusters in the Cell Membrane

We were interested in following the formation of active receptor complexes in the cell membrane and employed Gab1-EGFP as a tracer. For this purpose, we used the freeze-fracture replica immunogold-labeling method, an extension of freeze-fracture electron microscopy

[Fujimoto, 1997; Takizawa and Robinson, 2000], since it allows the in situ visualization of specific proteins and interactions within biomembranes. We studied the distribution of Gab1-EGFP NIH 5.15 in cells in dependence of NGF-induced Trk-Met activity. Cells were transiently transfected with both Trk-Met-BFP and Gab1-EGFP. Twenty-four hours post transfection they were split into halves and then either left untreated or stimulated with 50 ng/ml NGF for 30 min. They were cryofixed, freeze-fractured, and subjected to immuno-labeling with anti-Gab1 and gold-conjugated secondary antibody. Figure 2 shows comparative freeze-fracture views of the protoplasmic fracture face (PF) of

Molecular weights of marker proteins are given in kDa. For relative comparison of receptor tyrosine phosphorylation and expression, intensities of bands representing the mature form of Trk-Met-BFP (marked with asterisks) were scanned and quantified densitometrically (graphs below the upper two blots). **C:** Influence of transiently expressed Trk-Met-BFP and Gab1-EGFP on the invasive behavior of NIH 5.15 cells. Cells were either subjected to a transfection procedure in the absence of plasmid DNA or transfected with Trk-Met-BFP and Gab1-EGFP expression constructs individually or in combination as indicated. After a recovery period of 48 h post transfection, cells were transferred to medium devoid of serum for 24 h and optionally containing 50 ng/ml NGF and/or 1 μ g/ml doxycycline. Subsequently, samples of 2×10^5 cells were subjected to tests for migration through a Matrigel layer in transwell chambers as described in "Materials and Methods." The medium contained 50 ng/ml NGF if indicated.

Cells were transiently transfected with both Trk-Met-BFP and Gab1-EGFP. Twenty-four hours post transfection they were split into halves and then either left untreated or stimulated with 50 ng/ml NGF for 30 min. They were cryofixed, freeze-fractured, and subjected to immuno-labeling with anti-Gab1 and gold-conjugated secondary antibody.

Figure 2 shows comparative freeze-fracture views of the protoplasmic fracture face (PF) of

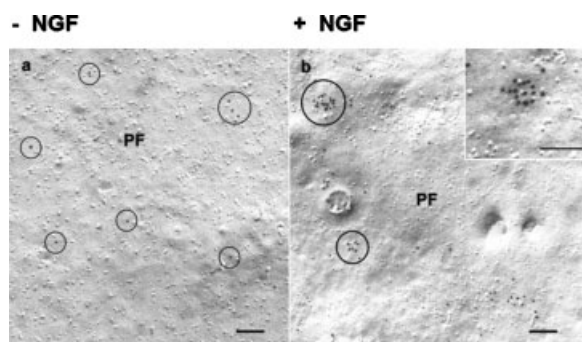


Fig. 2. Freeze-fracture micrographs of plasma membranes from chemically unfixed NIH 5.15 cells transiently expressing Trk-Met-BFP and Gab1-EGFP before (**left**) and after NGF stimulation (**right**). After SDS treatment, the protoplasmic fracture face (PF) was immunolabeled with anti-hGab1, indicating Gab1-d2eGFP molecules upon subsequent gold-labeling. For details see "Materials and Methods." Bars represent 100 nm.

plasma membranes from untreated and NGF-stimulated NIH 5.15 cells that had beforehand been transfected with Trk-Met-BFP and Gab1-EGFP. Gold particles (within the circles) indicate a nearly uniform distribution of Gab1-EGFP molecules in the membranes of untreated cells (Fig. 2A). The density of gold particles was 12 ± 4 particles per μm^2 membrane area. In some cases, small clusters of two or three particles were found. In contrast, addition of NGF to the cell culture resulted in a striking redistribution of Gab1-EGFP molecules into clusters (Fig. 2B). Up to 15 gold particles were counted in individual clusters (Fig. 2B, inset and within circles). NGF-stimulation increased the density of gold particles to 45 ± 16 particles per μm^2 membrane area.

Heterologous, Tagged c-Met Drives Anchorage-Independent and Invasive Growth of Fibroblasts

Next, we wished to demonstrate and quantify transforming properties of the fluorescence-tagged c-Met receptor complex. To assess long-term effects of oncogenic c-Met signaling on cell physiology, we generated a stable cell line expressing both Trk-Met-BFP and Gab1-EGFP by selection for hygromycin-resistant clones (see "Materials and Methods") and subsequent testing for expression by Western blot analysis employing an antibody to GFP. Abundance of both the hybrid receptor and Gab1 construct was clearly identifiable in about 30% of the clones analyzed, but by far weaker than in transient transfectants

(data not shown). One clone showing maximal expression of both proteins was chosen for further studies and termed NIH-TM-BFP/Gab1-EGFP.

First, we set out to demonstrate by biochemical means the stable abundance of the two heterologous fusion proteins. Due to the by far lower expression compared to transient transfection experiments, we found necessary to concentrate both proteins by immunoprecipitation before Western blot detection with antibodies to c-Met and Gab1. Figure 3A shows that both fluorescence-tagged fusion proteins could be precipitated and specifically detected in lysates of NIH-TM-BFP/Gab1-EGFP cells.

This stable cell line was next tested in a soft agar colony formation assay for its capability of growing anchorage independently in the presence and absence of NGF stimulation. Figure 3B shows that ligand-induced activation of the tagged c-Met receptor results in drastically enhanced colony formation, indicating receptor-dependent transformation.

As a second parameter of malignancy, we assayed the effect of NGF on the invasiveness of NIH-TM-BFP/Gab1-EGFP cells. In the course of this experiment, we also further examined the role of Gab1 in the control of c-Met-driven invasiveness (Fig. 3C). Expression of fluorescence-tagged hybrid receptor and Gab1 did already cause a slight increase in the rate at which NIH cells migrate through a layer of artificial extracellular matrix (Matrigel). Activation of the system by stimulation with NGF, however, led to an augmentation of invasiveness by about 50%, indicating full competence for oncogenic signal transduction. To address the contribution of Gab1 to c-Met-mediated invasiveness, we blocked expression of the Gab1-EGFP protein by employing the regulatable tet promoter and the "Tet-off" system intrinsic to NIH 5.15 cells. In the presence of 1 $\mu\text{g}/\text{ml}$ doxycycline Gab1-EGFP expression was reduced to trace amounts as verified by immunoprecipitations and Western blot (data not shown). Repression of Gab1-EGFP throughout invasion experiments resulted in a clear decrease of invasive cell behavior, both in the absence and presence of NGF-mediated c-Met activation. These results are consistent with those obtained in transient transfection experiments (Fig. 1C) and confirm the involvement of Gab1 in signaling pathways connecting c-Met to invasive cell migration.

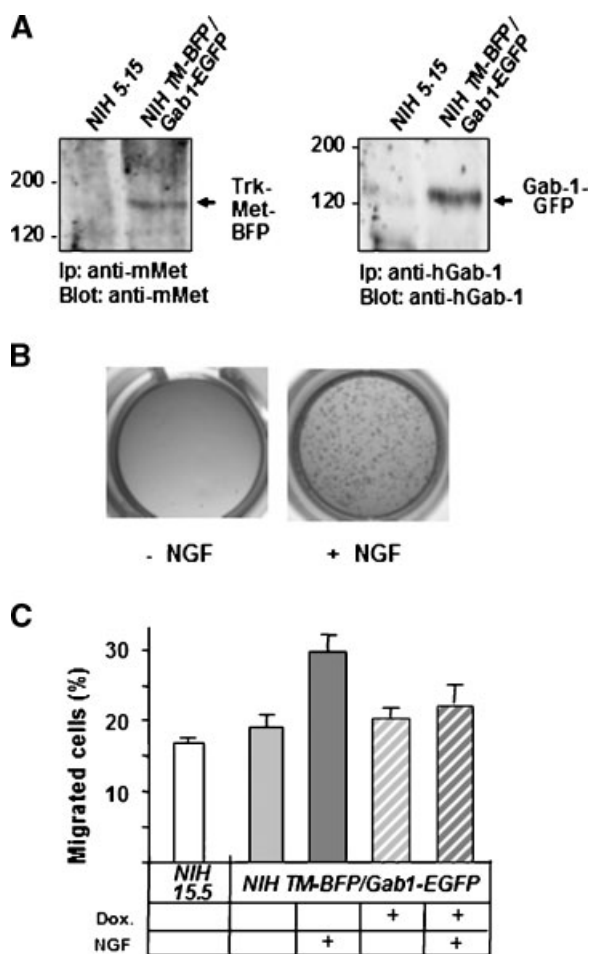


Fig. 3. Cell-transforming activity of the fluorescence-tagged c-Met-derived receptor complex. **A:** Stable expression of Trk-Met-BFP and Gab1-EGFP fusion proteins in NIH-TM-BFP/Gab1-EGFP cells. NIH 5.15 and NIH-TM-BFP/Gab1-EGFP cells were subjected to cell lysis, immunoprecipitation, and Western blot analysis as described in "Materials and Methods" employing antibodies to murine c-Met (**left**) and human Gab1 (**right**). **B:** Effect of NGF-mediated activation of the stably expressed heterogeneous receptor complex in NIH-TM-BFP/Gab1-EGFP cells on anchorage independent growth. Cells were subjected to a soft agar colony formation assay as described in "Materials and Methods" in the absence or presence of 50 ng/ml NGF as indicated. After 2 weeks of cultivation, colonies were stained and photographed. **C:** Influence of the Trk-Met-BFP and Gab1-EGFP expression on cell invasiveness. Non transfected NIH 5.15 cells or NIH-TM-BFP/Gab1-EGFP cells (the latter either in the absence or presence of 50 ng/ml NGF or/and 1 μ g/ml doxycycline as indicated) were tested for migration through a Matrigel layer in transwell chambers as described in "Materials and Methods." Results are expressed as the fraction of migrated cells in relation to the input and represent the means of three independent experiments.

c-Met Activates STAT3 in Fibroblasts

Other substrates of the c-Met receptor tyrosine kinase apart from Gab1 have been

implicated in motile and invasive cell behavior. The fact that we have recently identified STAT3, a potential oncoprotein implicated in various cancers, as an important determinant of invasiveness in choriocarcinoma cells [Corvinus et al., 2003] prompted us to study this factor in the context of c-Met-mediated cell transformation.

First we asked if STAT3, like Gab1, forms assemblies at the membrane of NIH 5.15 fibroblasts in response to ligand-induced activation of Trk-Met hybrid receptor. Cells transiently transfected with Trk-Met-BFP and Gab1-EGFP were left untreated or stimulated with 50 ng/ml NGF for 30 min. Upon cryofixation, they were freeze-fractured and immuno- and subsequently gold-labeled with an antibody to STAT3. Figure 4A shows a relatively equal distribution of gold particles indicating STAT3 molecules (marked by circles) on the membrane of non-stimulated cells. Interestingly, NGF treatment evoked the appearance of STAT3 clusters, a picture similar to that seen when probing the distribution of Gab1 (compare Fig. 2). This result is consistent with the view that STAT3 is recruited into receptor complex assemblies that form upon NGF-induced activation of the Trk-Met-BFP receptor.

To determine if STAT3 becomes activated via Trk-Met-BFP, we analyzed NIH 5.15 cells transiently transfected with Trk-Met-BFP, Gab1-EGFP, or both, for NGF-dependent tyrosine phosphorylation of STAT3. Figure 4B shows that expression of Trk-Met-BFP, either alone or in combination with Gab1-EGFP specifically evoked tyrosine phosphorylation of STAT3. In both cases, stimulation of transfectants with NGF further enhanced STAT3 phosphorylation. Anti-STAT3 (recognizing the aminoterminal of STAT3) reacted with an additional, smaller protein which represents STAT3 β , a splice variant lacking the carboxy terminus of full length STAT3 including Tyr 705, the target of activation-associated tyrosine phosphorylation [Caldenhoven et al., 1996].

siRNA-Mediated Knockdown of STAT3 Expression Abolishes c-Met-Induced Invasiveness of Fibroblasts

Recent findings on the involvement of STAT3 in tumorigenicity and cell motility prompted us to directly test its importance for c-Met-mediated invasiveness of fibroblasts. To this aim, we employed the NIH 5.15-derived cell line

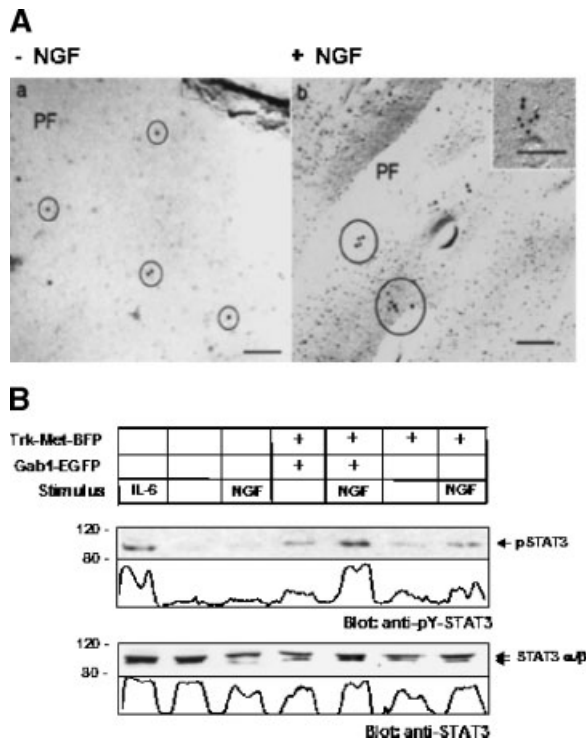


Fig. 4. Activation of STAT proteins through c-Met in fibroblasts. **A:** Analysis of STAT3 distribution in the membrane of fibroblasts. Freeze-fracture micrographs of anti-STAT3 labeled plasma membranes from chemically unfixated NIH 5.15 cells transiently expressing Trk-Met-BFP and Gab1-EGFP before (left) and after NGF stimulation (right). Immuno- and gold-labeling of protoplasmic fracture face (PF) with anti-STAT3 was performed analogous as in Figure 2. Bars represent 100 nm. **B:** Tyrosine phosphorylation of STAT3 in dependence of Trk-Met-BFP and Gab1-EGFP expression and NGF stimulation in NIH 5.15 cells. Cells were transiently transfected with the expression constructs and optionally treated with 50 ng/ml NGF for 30 min as indicated. Cell lysates were subjected to Western blotting and probed with an antibody to STAT3 phosphorylated on Tyrosine 705 (top). Comparability of protein amounts was verified by a parallel Western blot probed with anti-STAT3 (bottom). As a positive control for STAT3 activation, cells were treated for 30 min with 10 ng/ml human interleukin-6 (left hand lane). Molecular weights of marker proteins are given in kDa. For relative comparison of STAT3 tyrosine phosphorylation and expression, intensities of bands were scanned and quantified densitometrically (graphs below the blots).

stably expressing the fluorescence tagged Trk-Met/Gab1 complex (NIH-TM-BFP/Gab1-EGFP, see above). STAT3 was inhibited directly by pretreating cells with siRNAs, using a STAT3-specific sequence. As a specificity control, a “scrambled” sequence with the same base composition, but random sequence, was employed.

Equal numbers of cells were harvested from control cultures (non-transfected or transfected with “scrambled” (Scr) oligonucleotides) and from STAT3 siRNA-treated cultures 3 and

8 days post transfection. STAT3 expression was determined by Western blot analysis (Fig. 5A). Cells pretreated with 50 nM STAT3 siRNA showed a specific reduction in total STAT3 protein levels 3 days after transfection. The original level of STAT3 abundance was regained after 8 days. The suppressive effect was specifically elicited by the STAT3 siRNA and not by unspecific cell damage, since control (Scr) oligonucleotides had only a marginal effect on STAT3 expression.

In parallel, the ability of the siRNA-treated cells to invade extracellular matrix in the absence and presence of NGF stimulus was evaluated in transwell migration assays. Three days post transfection, a clear reduction in the migration of the STAT3 siRNA-treated cells both was observed compared with untreated and control transfected cells (Fig. 5B). Invasiveness in the absence of c-Met activation was reduced to about 70%, whereas invasiveness in response to NGF dropped to less than 50% of the original value. In fact, the invasiveness-promoting effect of NGF was completely

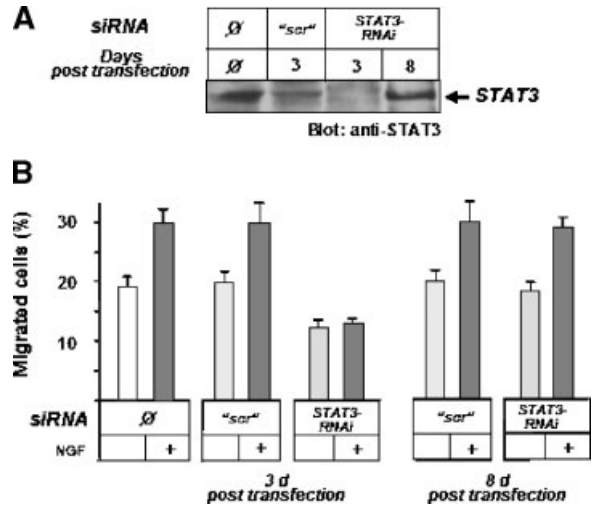


Fig. 5. Effect of siRNA-mediated STAT3 depletion on STAT3 expression and c-Met-induced invasiveness. NIH-TM-BFP/Gab1-EGFP cells were either left untreated or transfected with STAT3 siRNA or a “scrambled” control sequence as detailed in “Materials and Methods.” **A:** Comparison of STAT3 expression by Western blot analysis of non-transfected cells and cells treated with STAT3 siRNA or “scrambled” control. Cell lysates obtained 3 or 8 days post transfection were analyzed as indicated. **B:** Effect of STAT3 depletion on c-Met-mediated invasiveness of NIH-TM-BFP/Gab1-EGFP cells. Cells were either left untreated or transfected with STAT3 siRNA or “scrambled” control RNA as indicated. Three or 8 days post transfection, invasiveness in the absence or presence of 50 ng/ml NGF was determined as in Figure 3B.

abolished, indicating that c-Met-driven migration was entirely blocked.

Eight days after transfection, the original invasive potential of the cells was restored, both in the presence and absence of NGF stimulus. This recovery coincided with the return of STAT3 abundance and clearly argues for an important contribution of STAT3 signaling to the phenomenon of c-Met-driven invasive behavior of fibroblasts. Interestingly, even the basal invasiveness in the absence of NGF is inhibited when STAT3 is silenced. This presumably indicates a c-Met independent role for STAT3 in invasion. To exclude the possibility that the effect of STAT3 siRNA on invasiveness is a peculiarity of the stable cell line generated in this study, we made sure that knocking down STAT3 also reduces Trk-Met-driven invasiveness in the bulk of transiently transfected cells (data not shown).

DISCUSSION

Among its pleiotropic functions, transcription factor STAT3 is involved in the control of cell motility in several settings. Physiologically, STAT3 is crucial, e.g., for cell motility during gastrulation [Yamashita et al., 2002], wound healing [Sano et al., 1999; Kira et al., 2002], and blood vessel formation [Yahata et al., 2003].

Increased motility is one of the prerequisites for the invasiveness of tumor cells. Consistent with this notion, inadequate activity of STAT3 was found correlated with cancer-associated motility of breast [Badache and Hynes, 2001] and ovarian cancer cells [Silver et al., 2004]. Cell migration is influenced by focal adhesions which are thought to transduce extracellular signals into changes in cell adhesion, status of the cytoskeleton, and gene expression. One possible role of STAT3 in the promotion of motility may lie in its emerging function as a signaling adaptor at focal adhesions and, presumably, as a persistent scaffold factor in cytokine/growth factor receptor assemblies. In ovarian cancer cells, activated STAT3 was localized not only to nuclei but also to focal adhesions, where it displayed interactions with paxillin as well as with Src and focal adhesion kinase p125FAK [Silver et al., 2004]. An involvement of STAT proteins in the function and signal transduction of focal adhesions is apparently not restricted to STAT3, since STAT1 has also been shown to be tyrosine

phosphorylated by focal adhesion kinase in the course of integrin-mediated cell migration and adhesion [Xie et al., 2001]. It has been shown that c-Met-triggered cell migration involves the initial recruitment of integrins, cytoskeletal proteins, and p125FAK into a complex [Matsumoto et al., 1994; Parr et al., 2001], and colocalization of integrins and growth factor receptors are discussed to provide specific signaling environments [Baron et al., 2003]. In this study, we have obtained direct evidence for the formation of multiprotein assemblies within the membrane in the course of c-Met activation. Importantly, the employed technique of immuno-electron microscopy on freeze-fracture replicas allows for the visualization of protein clusters after cryofixation of native samples, avoiding any diffusion of target molecules after fixation. Further exploiting the potential of the method should enable us to determine if indeed c-Met, focal adhesion kinase and STAT3 get into close contact upon ligand-induced activation of the c-Met tyrosine kinase.

An additional important aspect of invasiveness is the expression of proteases that render the invasive cells capable of digesting constituents of the extracellular matrix. Various reports point to a role of STAT3 in promoting invasive cell behavior by exerting influence on the transcription of protease genes. In metastatic melanoma cells, the expression of matrix metalloproteinase (MMP)-2 as well as invasiveness was found connected with constitutive STAT3 activity. Importantly, inhibition of STAT3 by a dominant-negative mutant reduced MMP-2 expression and invasiveness and blocked metastasis in nude mice [Xie et al., 2004]. In epithelial cells of the skin, STAT3 was shown to mediate the IL-6-induced induction of MMP-1 and MMP-3 [Yu et al., 2002]. STAT3 is involved in the expression control of MMP-7 in prostate carcinoma cells [Udayakumar et al., 2002] and of MMP-9 in cervix carcinoma cells [Smola-Hess et al., 2001]. The MMP-1 promoter contains a STAT binding site with importance for oncostatin M-induced MMP-1 expression [Korzus et al., 1997]. We have shown recently that STAT3 directly drives transcription from the MMP-1 promoter in colon carcinoma cells (manuscript in preparation).

We suggest that STAT3 can generally contribute to cell motility and tumor progression. It does so in a cell-type- and situation-specific manner by influencing both cell adhesion and

the expression of genes with relevance for invasive growth. Tumor promoting activity of STAT3 can arise either via inadequately activated cytokine and growth factor receptors, or by phosphorylation through kinases such as Src or focal adhesion kinase, both of which are involved in focal adhesion turnover and dynamics. Disturbed equilibrium of nuclear and adapter functions, e.g., in focal adhesion of STAT3 may be responsible for the cell transforming outcome in one or the other way. It is consistent with this view, that suppressing the function of STAT3 by a dominant-negative mutant in a colon carcinoma cell line abolished its dependency on HGF/c-Met signaling for invasive growth. Moreover, it increased tyrosine phosphorylation of the cell adhesion regulator beta-catenin and its dissociation from the invasion suppressor E-cadherin [Rivat et al., 2004].

Taken together, STAT3 is obviously involved in the control of cell motility and invasiveness in various important ways. Exploiting its potential as a target for anti-tumor drugs, however, requires a better understanding of the cell type and situation-specific role of STAT3 in cellular malignancy.

ACKNOWLEDGMENTS

We thank Martin Sachs and Jakob Troppmair for the gift of plasmids and cells, Tobias Poehlmann and Udo Markert for the collaboration on siRNA-mediated STAT3 knockdown, and Bernd Wiederanders for valuable discussions.

REFERENCES

- Atabey N, Gao Y, Yao ZJ, Breckenridge D, Soon L, Soriano JV, Burke TR, Jr., Bottaro DP. 2001. Potent blockade of hepatocyte growth factor-stimulated cell motility, matrix invasion and branching morphogenesis by antagonists of grb2 src homology 2 domain interactions. *J Biol Chem* 276:14308–14314.
- Badache A, Hynes NE. 2001. Interleukin 6 inhibits proliferation and, in cooperation with an epidermal growth factor receptor autocrine loop, increases migration of T47D breast cancer cells. *Cancer Res* 61:383–391.
- Baron W, Decker L, Colognato H, Iffrench-Constant C. 2003. Regulation of integrin growth factor interactions in oligodendrocytes by lipid raft microdomains. *Curr Biol* 13:151–155.
- Boccaccio C, Ando M, Tamagnone L, Bardelli A, Michieli P, Battistini C, Comoglio PM. 1998. Induction of epithelial tubules by growth factor HGF depends on the STAT pathway. *Nature* 391:285–288.
- Bromberg JF, Wrzeszczynska MH, Devgan G, Zhao Y, Pestell RG, Albanese C, Darnell JE, Jr. 1999. Stat3 as an oncogene. *Cell* 98:295–303.
- Caldenhoven E, van Dijk TB, Solari R, Armstrong J, Raaijmakers JA, Lammers JW, Koenderman L, de Groot RP. 1996. STAT3beta, a splice variant of transcription factor STAT3, is a dominant negative regulator of transcription. *J Biol Chem* 271:13221–13227.
- Corvinus FM, Fitzgerald JS, Friedrich K, Markert UR. 2003. Evidence for a correlation between trophoblast invasiveness and STAT3 activity. *Am J Reprod Immunol* 50:316–321.
- Dhir R, Ni Z, Lou W, DeMiguel F, Grandis JR, Gao AC. 2002. Stat3 activation in prostatic carcinomas. *Prostate* 51:241–246.
- Friedrich K, Wietek S. 2001. Experimental regulation of STAT expression reveals an involvement of STAT5 in interleukin-4-driven cell proliferation. *Biol Chem* 382:343–351.
- Fujimoto K. 1997. SDS-digested freeze-fracture replica labeling electron microscopy to study the two-dimensional distribution of integral membrane proteins and phospholipids in biomembranes: Practical procedure, interpretation and application. *Histochem Cell Biol* 107:87–96.
- Garcia R, Bowman TL, Niu G, Yu H, Minton S, Muro-Cacho CA, Cox CE, Falcone R, Fairclough R, Parsons S, Laudano A, Gazit A, Levitzki A, Kraker A, Jove R. 2001. Constitutive activation of Stat3 by the Src and JAK tyrosine kinases participates in growth regulation of human breast carcinoma cells. *Oncogene* 20:2499–2513.
- Gresch O, Engel FB, Nestic D, Tran TT, England HM, Hickman ES, Korner I, Gan L, Chen S, Castro-Obrigon S, Hammermann R, Wolf J, Müller-Hartmann H, Nix M, Siebenkotten G, Kraus G, Lun K. 2004. New non-viral method for gene transfer into primary cells. *Methods* 33:151–163.
- Horiguchi A, Oya M, Shimada T, Uchida A, Marumo K, Murai M. 2002. Activation of signal transducer and activator of transcription 3 in renal cell carcinoma: A study of incidence and its association with pathological features and clinical outcome. *J Urol* 168:762–765.
- Jeffers M, Rong S, Vande Woude GF. 1996. Hepatocyte growth factor/scatter factor-Met signaling in tumorigenicity and invasion/metastasis. *J Mol Med* 74:505–513.
- Kammer W, Lischke A, Moriggl R, Groner B, Ziemiecki A, Gurniak CB, Berg LJ, Friedrich K. 1996. Homodimerization of interleukin-4 receptor alpha chain can induce intracellular signalling. *J Biol Chem* 271:23634–23637.
- Kerkhoff E, Houben R, Löffler S, Troppmair J, Lee JE, Rapp UR. 1998. Regulation of c-myc expression by Ras/Raf signalling. *Oncogene* 16:211–216.
- Kira M, Sano S, Takagi S, Yoshikawa K, Takeda J, Itami S. 2002. STAT3 deficiency in keratinocytes leads to compromised cell migration through hyperphosphorylation of p130(cas). *J Biol Chem* 277:12931–12936.
- Korzus E, Nagase H, Rydell R, Travis J. 1997. The mitogen-activated protein kinase and JAK-STAT signaling pathways are required for an oncostatin M-responsive element-mediated activation of matrix metalloproteinase 1 gene expression. *J Biol Chem* 272:1188–1196.
- Kotelevts L, Noe V, Bruyneel E, Myssiakine E, Chastre E, Mareel M, Gaspach C. 1998. Inhibition by platelet-activating factor of Src- and hepatocyte growth factor-dependent invasiveness of intestinal and kidney epithelial cells. Phosphatidylinositol 3'-kinase is a critical mediator of tumor invasion. *J Biol Chem* 273:14138–14145.

- Levy DE, Lee CK. 2002. What does Stat3 do? *J Clin Invest* 109:1143–1148.
- Li W, Michieli P, Alimandi M, Lorenzi MV, Wu Y, Wang LH, Heidarman MA, Pierce JH. 1996. Expression of an ATP binding mutant of PKC-delta inhibits Sis-induced transformation of NIH3T3 cells. *Oncogene* 13:731–737.
- Li J, Xia F, Li WX. 2003. Coactivation of STAT and Ras is required for germ cell proliferation and invasive migration in *Drosophila*. *Dev Cell* 5:787–798.
- Lischke A, Kammer W, Friedrich K. 1995. Different human interleukin-4 mutants preferentially activate human or murine common receptor gamma chain. *Eur J Biochem* 234:100–107.
- Lock LS, Royall I, Naujokas MA, Park M. 2000. Identification of an atypical Grb2 carboxyl-terminal SH3 domain binding site in Gab docking proteins reveals Grb2-dependent and -independent recruitment of Gab1 to receptor tyrosine kinases. *J Biol Chem* 275:31536–31545.
- Maroun CR, Holgado-Madruga M, Royall I, Naujokas MA, Fournier TM, Wong AJ, Park M. 1999. The Gab1 PH domain is required for localization of Gab1 at sites of cell-cell contact and epithelial morphogenesis downstream from the met receptor tyrosine kinase. *Mol Cell Biol* 19:1784–1799.
- Matsumoto K, Nakamura T, Kramer RH. 1994. Hepatocyte growth factor/scatter factor induces tyrosine phosphorylation of focal adhesion kinase (p125FAK) and promotes migration and invasion by oral squamous cell carcinoma cells. *J Biol Chem* 269:31807–31813.
- Otsuka T, Takayama H, Sharp R, Celli G, LaRochelle WJ, Bottaro DP, Ellmore N, Vieira W, Owens JW, Anver M, Merlino G. 1998. c-Met autocrine activation induces development of malignant melanoma and acquisition of the metastatic phenotype. *Cancer Res* 58:5157–5167.
- Parr C, Davies G, Nakamura T, Matsumoto K, Mason MD, Jiang WG. 2001. The HGF/SF-induced phosphorylation of paxillin, matrix adhesion, and invasion of prostate cancer cells were suppressed by NK4, an HGF/SF variant. *Biochem Biophys Res Commun* 285:1330–1337.
- Ponzetto C, Bardelli A, Zhen Z, Maina F, dalla Zonca P, Giordano S, Graziani A, Panayotou G, Comoglio PM. 1994. A multifunctional docking site mediates signaling and transformation by the hepatocyte growth factor/scatter factor receptor family. *Cell* 77:261–271.
- Rahimi N, Hung W, Tremblay E, Saulnier R, Elliott B. 1998. c-Src kinase activity is required for hepatocyte growth factor-induced motility and anchorage-independent growth of mammary carcinoma cells. *J Biol Chem* 273:33714–33721.
- Rivat C, Wever OD, Bruyneel E, Mareel M, Gaspach C, Attoub S. 2004. Disruption of STAT3 signaling leads to tumor cell invasion through alterations of homotypic cell-cell adhesion complexes. *Oncogene* 23:3317–3327.
- Rong S, Segal S, Anver M, Resau JH, Vande Woude GF. 1994. Invasiveness and metastasis of NIH 3T3 cells induced by Met-hepatocyte growth factor/scatter factor autocrine stimulation. *Proc Natl Acad Sci USA* 91:4731–4735.
- Rubin JS, Bottaro DP, Aaronson SA. 1993. Hepatocyte growth factor/scatter factor and its receptor, the c-met proto-oncogene product. *Biochem Biophys Acta* 1155:357–371.
- Sachs M, Weidner KM, Brinkmann V, Walther I, Obermeier A, Ullrich A, Birchmeier W. 1996. Motogenic and morphogenic activity of epithelial receptor tyrosine kinases. *J Cell Biol* 133:1095–1107.
- Sano S, Itami S, Takeda K, Tarutani M, Yamaguchi Y, Miura H, Yoshikawa K, Akira S, Takeda J. 1999. Keratinocyte-specific ablation of Stat3 exhibits impaired skin remodeling, but does not affect skin morphogenesis. *EMBO J* 18:4657–4668.
- Schaefer LK, Ren Z, Fuller GN, Schaefer TS. 2002. Constitutive activation of Stat3alpha in brain tumors: Localization to tumor endothelial cells and activation by the endothelial tyrosine kinase receptor (VEGFR-2). *Oncogene* 21:2058–2065.
- Silver DL, Naora H, Liu J, Cheng W, Montell DJ. 2004. Activated signal transducer and activator of transcription (STAT) 3: Localization in focal adhesions and function in ovarian cancer cell motility. *Cancer Res* 64:3550–3558.
- Smola-Hess S, Schnitzler R, Hadaschik D, Smola H, Mauch C, Krieg T, Pfister H. 2001. CD40L induces matrix-metalloproteinase-9 but not tissue inhibitor of metalloproteinases-1 in cervical carcinoma cells: Imbalance between NF-kappaB and STAT3 activation. *Exp Cell Res* 267:205–215.
- Takizawa T, Robinson JM. 2000. Freeze-fracture cytochemistry: A new fracture-labeling method for topological analysis of biomembrane molecules. *Histol Histopathol* 15:515–522.
- Udayakumar TS, Stratton MS, Nagle RB, Bowden GT. 2002. Fibroblast growth factor-1 induced promatrilysin expression through the activation of extracellular-regulated kinases and STAT3. *Neoplasia* 4:60–67.
- Weidner KM, Di Cesare S, Sachs M, Brinkmann V, Behrens J, Birchmeier W. 1996. Interaction between Gab1 and the c-Met receptor tyrosine kinase is responsible for epithelial morphogenesis. *Nature* 384:173–176.
- Wells A, Kassis J, Solava J, Turner T, Lauffenburger DA. 2002. Growth factor-induced cell motility in tumor invasion. *Acta Oncol* 41:124–130.
- Xie B, Zhao J, Kitagawa M, Durbin J, Madri JA, Guan J-L, Fu X-Y. 2001. Focal adhesion kinase activates Stat1 in integrin-mediated cell migration and adhesion. *J Biol Chem* 276:19512–19523.
- Xie TX, Wei D, Liu M, Gao AC, Ali-Osman F, Sawaya R, Huang S. 2004. Stat3 activation regulates the expression of matrix metalloproteinase-2 and tumor invasion and metastasis. *Oncogene* 23:3550–3560.
- Yahata Y, Shirakata Y, Tokumaru S, Yamasaki K, Sayama K, Hanakawa Y, Detmar M, Hashimoto K. 2003. Nuclear translocation of phosphorylated STAT3 is essential for vascular endothelial growth factor-induced human dermal microvascular endothelial cell migration and tube formation. *J Biol Chem* 278:40026–40031.
- Yamashita S, Miyagi C, Carmany-Rampey A, Shimizu T, Fujii R, Schier AF, Hirano T. 2002. Stat3 controls cell movements during zebrafish gastrulation. *Dev Cell* 2:363–375.
- Yu CY, Wang L, Khaletskiy A, Farrar WL, Larner A, Colburn NH, Li JJ. 2002. STAT3 activation is required for interleukin-6 induced transformation in tumor-promotion sensitive mouse skin epithelial cells. *Oncogene* 21:3949–3960.
- Zhang YW, Wang LM, Jove R, Vande Woude GF. 2002. Requirement of Stat3 signaling for HGF/SF-Met mediated tumorigenesis. *Oncogene* 21:217–226.